

Synthesis and Research on Photocatalytic Activity of ZIF-8 Derived ZnO/CdS Copolymer Photocatalyst

Kaiqiang Mou, Min Zhu, Huimin Xu and Yan Xie ^a

School of Chemical Engineering and Safety, Binzhou University, Binzhou 256603, China;

^azbuxie@163.com

Abstract

In this work, a series of ZIF-8 derived ZnO/CdS composite photocatalysts were successfully prepared by pyrolysis based on a zinc-based zeolite imidazole frameworks (ZIFs), loaded on ZIF-8 with cadmium acetate dehydrate as cadmium source and thiourea as sulfur source. All photocatalytic samples were characterized by XRD, SEM, TEM, and UV-vis diffuse reflectance spectra. The influence of ZIF-8 derived ZnO/CdS on the photocatalytic activity of rhodamine B (RhB) has been investigated under simulated sunlight irradiation. The results detect that ZIF-8 was completely converted into ZnO when it was calcined at 540 °C for 8 hours under air atmosphere, and CdS was well dispersed onto ZnO surface. The photocatalytic efficiency of ZnO is only 76.65%, while photocatalytic efficiency of ZIF-8 derived ZnO/CdS was highly improved (99.7%). Furthermore, ZIF-8 derived ZnO/CdS exhibited high photocatalytic activity and stability. After four cycles of repeated application, the photocatalytic efficiency of ZIF-8 derived ZnO/CdS was highly retained at 96.56%.

Keywords

ZIF-8; CdS; ZnO; Rhodamine B; Photocatalysts.

1. Introduction

Over the past decades, serious water pollution issues and energy crisis were of great concern around worldwide, semiconductor photocatalysts have attracted more and more scientific attention due to its simple process, high efficiency and environment friendly [1-3]. To date, a large mass of semiconductor photocatalysts have been carried out for solar energy transformation and dispose of organic pollutants, for example TiO₂ [4], ZnO [5], SnO₂ [6], CdS [7], and BiVO₄ [8]. Among all of these semiconductors, ZnO has been caused considerable scientific interest as a substitute for TiO₂ photocatalyst because of its eco-friendly, high photocatalytic stability and photodegradation efficiency. However, pristine ZnO still has many defects in practical application process, which are low visible light utilization efficiency (because of a wide band gap 3.27 eV), rapid recombination rate of photo-induced electron-hole pairs, and low specific surface area. In order to overcome these shortcomings, a large of efforts have been made to improve its photocatalytic efficiency, such as metal or non-metal element doping [9-10], semiconductor photocatalyst coupling [11], self-assembly [12], and regulating template method [13]. Among above these methods, the template method of ZIF-8 derived ZnO can not only resolve the problem of low visible light utilization efficiency and rapid electron-hole pair recombination ratio but also upgrade the drawback of low specific surface area.

In this work, ZnO particle derived ZIF-8 was prepared by calcination with the template method of ZIF-8, loaded on surface of ZIF-8 derived ZnO with CdS nanoparticles. Then, the photodegradation activity of all samples was performed by using rhodamine B as simulated pollutant in aqueous solution under simulated sunlight radiation. After detailed studying, ZIF-8 derived ZnO/CdS

composite photocatalysts exhibit higher photodegradation activity than the pristine ZnO nanoparticle derived from ZIF-8. ZIF-8 derived ZnO/CdS photocatalysts are expected to have potential application value in the degradation of some organic dyes under simulated sunlight driven in the future.

2. Experimental section

2.1 Chemicals and drugs

Zinc nitrate hexahydrate, cadmium diacetate dehydrate, methanol, ethyl alcohol, 2-Methylimidazole, rhodamine B (RhB) and thioacetamide were purchased from Shanghai Aladdin Chemical Reagent Co. Ltd. All chemicals and drugs were level of AR and used directly without any further purification. Distilled water was employed throughout all the experiments.

2.2 Synthesis of ZIF-8 derived ZnO/CdS composite photocatalysts

The ZIF-8 derived ZnO/CdS composite photocatalysts was synthesized by pyrolysis with the template method of ZIF-8. The synthesized procedures include the synthesis of ZIF-8, ZnO derived from ZIF-8, and resemble of the CdS loaded on the surface of ZnO.

ZIF-8 was synthesized using modified reference method. Firstly, 10 mmol $\text{Zn}(\text{NO}_3)_2 \cdot 6\text{H}_2\text{O}$ and 40 mmol of 2-methylimidazole respectively were dissolved in 100 mL of methanol to form clear solution. Then, the $\text{Zn}(\text{NO}_3)_2 \cdot 6\text{H}_2\text{O}$ solution was dropwise added into the 2-methylimidazole solution with vigorous stirring. Subsequently, the mixture was aged for 24 h at room temperature. Finally, the product was centrifuged, washed with distilled water and methanol successively, dried at 75 °C under vacuum oven for 10 h, and obtained ZIF-8.

ZnO derived from ZIF-8 was calcined at 540 °C for 8 hours to remove the organic residue, and obtain the ZIF-8 derived ZnO.

The ZIF-8 derived ZnO/CdS composite photocatalysts was synthesized with the template method of ZIF-8 by the following method. Typically, 50 mg of ZnO derived from ZIF-8 was dispersed in 20 mL of methanol to form a uniform dispersion system, labeled as A solution. Then, 8.1 mg of $\text{Cd}(\text{CH}_3\text{COO})_2 \cdot 2\text{H}_2\text{O}$ and 4.6 mg thioacetamide respectively were slowly added to A solution under continuous stirring, react at 75 °C for 30 mins. After that, the mixture was filtered and washed with ethanol for several times to remove the residual Cd^{2+} and organic species. Finally, the sample was dried under vacuum oven at 75 °C for 12 h, and obtained ZIF-8 derived ZnO/CdS composite photocatalyst. The different mass of ZIF-8 derived ZnO/CdS composite photocatalyst was obtained according the above synthesis procedure, which 5% ZIF-8 derived ZnO/CdS, 10% ZIF-8 derived ZnO/CdS, 30% ZIF-8 derived ZnO/CdS respectively labeled as ZCS-1, ZCS-2 and ZCS-3.

2.3 Characterization of the photocatalyst

X-ray powder diffraction (XRD) crystal structure of photocatalyst was carried out on a Bruker D/max-2500 diffractometer using $\text{Cu K}\alpha$ radiation, scanned in the angular range (2θ) from 5 to 75° at 40kV and 40 mA. Scanning electron microscopy (SEM) was measured on Hitachi S-4800 field emission to investigate the morphologies of photocatalyst. The UV-vis diffuse-reflectance spectra (UV-vis DRS) were performed on Beijing PERSEE TU-1905 Ultraviolet spectrophotometer.

2.4 Photocatalytic degradation experiment

The Photocatalytic degradation experiment of all the samples was carried out on CEL-LB70-3 photochemical reaction box under simulated sunlight irradiation, and evaluated by a concentration of 1 mg/L rhodamine B (RhB) as a simulated pollutant. In photodegradation experiment, 20 mg as-synthesized products were dispersed in 50 mL RhB aqueous solution with magnetic stirring. Then, the solution was kept in dark for 30 min under continuous stirring to attain the adsorption and desorption equilibrium. Afterwards, the RhB solutions were irradiated with a 350 W Xe lamp (with a 420nm UV-cutoff filter) at 30 min intervals.

3. Results and discussion

3.1 XRD Analysis

The X-ray diffraction (XRD) patterns of all the samples are shown in Fig.1. Fig.1 shows that the diffraction of pristine ZIF-8 sample well conforms to the characteristic diffraction pattern in references [14-15]. Thus, ZIF-8 is successfully synthesized. After ZIF-8 is calcined at 540 °C for 8 hours, the X-ray diffraction of ZnO derived from ZIF-8 suggests that the original peaks matching to ZIF-8 are no longer exhibit in Fig.1b. Fig. 1c shows the XRD pattern of 10% ZIF-8 derived ZnO/CdS photocatalytic composite. It can be seen that new peaks at 26.45°, 43.87° and 51.96° are ascribable to the (111), (220) and (311) reflections of CdS (JCPDS65-2887), respectively. These results suggest that CdS nanoparticles is well dispersed onto the surface of ZnO.

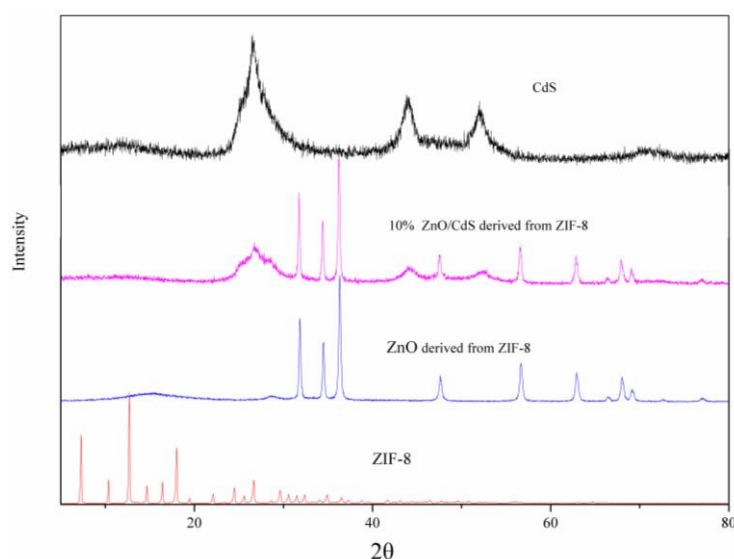


Fig 1 XRD patterns of the samples

3.2 SEM Analysis

The morphology and structure of all the samples was measured by the SEM (Fig. 2a-2d). As shown in Fig. the as-prepared ZIF-8 exhibits regular dodecahedral morphology. While ZIF-8 is calcined at 540 °C for 8 hours, its framework is collapsed (Fig. 2b), and the size of ZnO particle decreases from 250 nm to 100nm. When CdS nanoparticles is loaded onto ZnO derived from ZIF-8, the surface of ZnO particle is coated by CdS nanoparticles from Fig. 2d. The results indicate that CdS nanoparticles were embedded on the surface of ZnO. Furthermore, Fig. 3 depicts the EDS mappings of ZnO/CdS, the EDS images suggest the existence of the elements Zn, O, Cd and S. CdS nanoparticle is well dispersed on the surface of ZnO. This confirms that the organic ligands of ZIF-8 calcined at 540 °C for 8 hours are absolutely burned out.

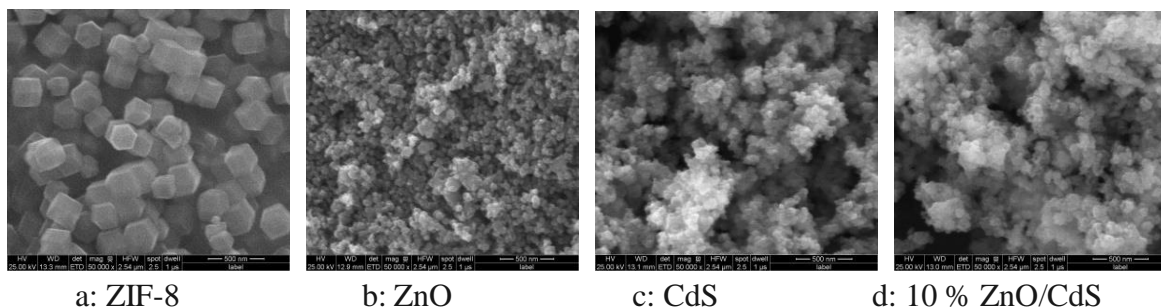


Fig. 2 SEM of all the samples

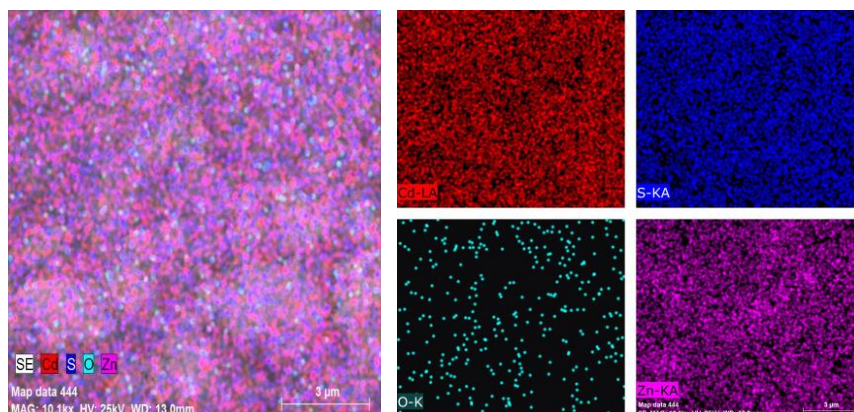


Fig. 3 Mapping of ZIF-8 derived 10% ZnO/CdS

3.3 UV-vis DRS Analysis

The UV-vis diffuse reflectance spectroscopy (DRS) of all the samples is shown in Fig .4. The spectra of ZIF-8 depicts a sharp peak nearly at 252 nm, which is consistent with the reference [16-17], ascribed to the excitonic absorption of ZIF-8. Nevertheless, after ZIF-8 is calcined at 540 °C for 8 hours, it shows a strong absorption peak at 388 nm. This suggests that ZnO is completely obtained from ZIF-8 by calcination at 540 °C. When ZnO is coupled with CdS nanoparticle by hydrothermal method, its characteristic absorption shows an obviously red shift, corresponding both to ZnO and CdS, which is probably attributed to the strong interfacial coupling effect between the neighbouring ZnO and CdS nanoparticles.

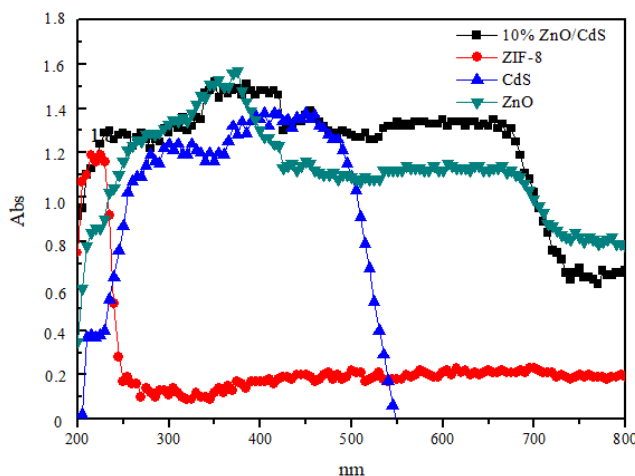


Fig. 4 UV-vis spectra of the samples

3.4 Photocatalytic Activity

The photocatalytic activity of all the samples was carried out using the degradation of an RhB solution as a simulated pollutant under simulated sunlight irradiation. The results are depicted in Fig. 5. It can be seen from Fig. 5 that 55.67% of RhB was adsorbed by ZIF-8, and only 17.12% and 16.34% of RhB were respectively adsorbed by ZnO and CdS/ZnO, after 30 min of dark reaction. Then, they were irradiated under simulated sunlight. After 60 min of irradiation, only 12.57% of RhB was degraded under no photocatalyst. ZIF-8 displayed almost no degradation properties, ZnO could degrade 76.65% of RhB, and the photocatalytic efficiency of CdS/ZnO was 99.7%. This shows that coupling with CdS could highly increase the photocatalytic activity of ZnO.

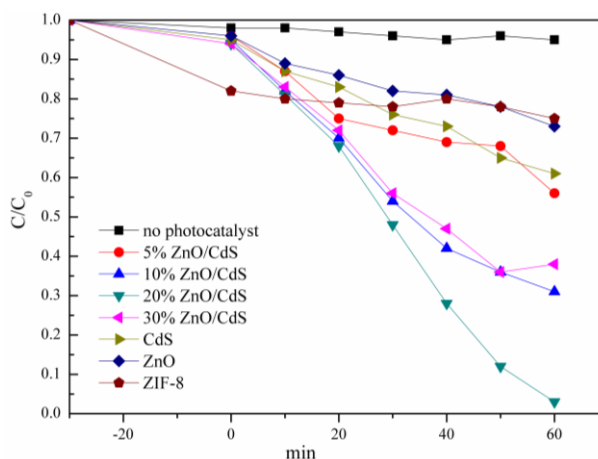


Fig. 5 The photocatalytic degradation of the samples, for the absorption of RhB in the dark and degradation of RhB under simulated sunlight irradiation

In order to certify the photocatalytic recycling stability of the as-synthesized photocatalyst, ZnO/CdS was performed to degrade RhB experiment for four photocatalytic degradation cycles under simulated sunlight. As can be seen from Fig. 6, after four photocatalytic degradation cycles the photocatalytic efficiency of ZnO/CdS decreases by just 3.16%. This suggests that ZnO/CdS shows high photocatalytic recycling stability. The slight decrease in photodegradation effect is probably attributed to the active sites of the composite photocatalyst occupied by intermediate products or reaction products generated by the reaction in the photodegradation process, thus blocking the action of simulated sunlight and the photocatalyst [19-20].

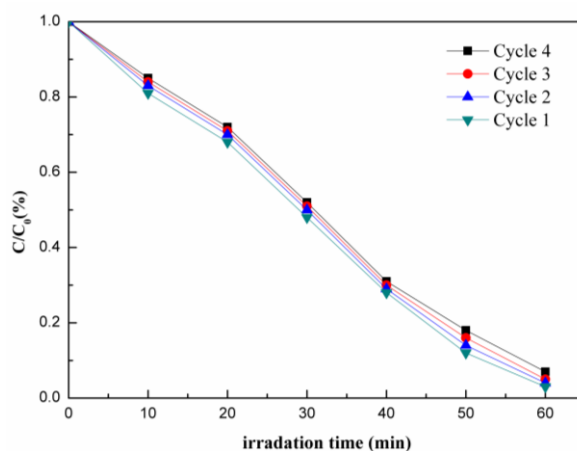


Fig. 6 Four photocatalytic degradation cycles of RhB using 10% ZnO/CdS

4. Conclusion

In summary, CdS nanoparticles loaded on surface of ZnO, with enhanced photocatalytic activity, was prepared from a ZIF-8 precursor through an hydrothermal method. CdS nanoparticles were well dispersed onto ZnO surface, which was synthesized from ZIF-8. Compared with that of ZIF-8, the photodegradation activity has been successfully upgraded under simulated sunlight irradiation. The results of degradation RhB show that the photocatalytic efficiency of ZnO was increased from 76.65% to 99.70% after CdS coupled with ZnO. Furthermore, ZnO/CdS depicts high photocatalytic stability. After four photocatalytic degradation cycles, the photocatalytic efficiency of ZnO/CdS was still highly maintained at 96.56%. It is suggested that the excellent photocatalytic properties of ZnO/CdS make it possible to be utilized for the degradation of organic pollutants.

5. Conflicts of interest

All authors declared to no conflicts in this work.

Acknowledgements

All the authors gratefully acknowledge the financial support of the National Natural Science Foundation of China (51801013), the Scientific Research Fund of Binzhou University (2016Y07), and the College Students Innovation & Entrepreneurship Program in Shandong Province (S201910449033).

References

- [1] A. Fujishima, K. Honda, Electrochemical Photolysis of Water at a Semiconductor Electrode, *Nature*, Vol. 238 (1972), P. 37-38.
- [2] J. H. Kennedy, K. W. Frese, Photo-oxidation of Water at Barium Titanate Electrodes. *Electrochem Soc*, Vol. 23 (1976), P. 1683-1686.
- [3] Y. Zhang, J. Zhou, W. Cai, J. Zhou, Z. Li, Enhanced photocatalytic performance and degradation pathway of Rhodamine B over hierarchical double-shelled zinc nickel oxide hollow sphere heterojunction, *Appl. Surf. Sci.*, Vol. 430(2018), P. 549-560.
- [4] S. U. M. Khan, M. Al-Shahry, W. B. Ingler, Efficient Photochemical Water Splitting by a Chemically Modified n-TiO₂, *Science*, Vol. 297 (2002), P. 2243-2245.
- [5] F. Xu, Y. T. Shen, L. T. Sun, H. B. Zeng and Y. N. Lu, Enhanced photocatalytic activity of hierarchical ZnO nanoplate-nanowire architecture as environmentally safe and facilely recyclable photocatalyst, *Nanoscale*, Vol. 3 (2011), P. 5020-5025
- [6] Z. Dai, J. Gole, J. Stout and Z. Wang, Tin Oxide Nanowires, Nanoribbons, and Nanotubes, *J. Phys. Chem. B*, Vol. 106 (2002), P. 1274-1279.
- [7] T. Gao, Q. Li and T. Wang, CdS nanobelts as photoconductors, *Appl. Phys. Lett*, Vol. 86 (2005), P. 173105.
- [8] G. Q. Tan, L. L. Zhang, H. J. Ren, S. S. Wei, J. Huang, A. Xia, Effects of pH on the hierarchical structures and photocatalytic performance of BiVO₄ powders prepared via the microwave hydrothermal method, *Appl. Mater. Interfaces*, Vol. 5 (2013), P. 5186-5193.
- [9] D. Zhang, Y. Zhao, L. Chen, Fabrication and characterization of amino-grafted graphene oxide modified ZnO with high photocatalytic activity, *Appl. Surf. Sci.*, Vol. (2018), P. 638-647.
- [10] L. P. Zheng, X. W. Li, W. C. Du, D. W. Shi, W. S. Ning, X. Y. Lu, Z. Y. Hou, Metal-organic framework derived Cu/ZnO catalysts for continuous hydrogenolysis of glycerol, *Appl. Catal. B: Environ*, Vol. 203 (2017), P. 146-153.
- [11] S. W. Zhao, H. F. Zuo, Y. R. Guo, Q. J. Pan, Carbon-doped ZnO aided by carboxymethyl cellulose: Fabrication, photoluminescence and photocatalytic applications, *J. Alloys Compd*, Vol. 695 (2017), P. 1029-1037.
- [12] S. Wang, X. Zhang, S. Li, Y. Fang, L. Pan, J. J. Zou, C-doped ZnO ball-in-ball hollow microspheres for efficient photocatalytic and photoelectrochemical applications, *J. Hazard. Mater*, Vol. 331 (2017), P. 235-245.
- [13] Y. Song, Y. Chen, J. Wu, Y. Fu, R. Zhou, S. Chen, L. Wang, Hollow metal organic frameworks-derived porous ZnO/C nanocages as anode materials for lithium-ion batteries, *J. Alloys. Compd*. Vol. 694 (2017), P. 1246-1253.
- [14] L. H. Wee, N. Janssens, S. P. Sree, C. Wiktor, E. Gobechiya, R. A. Fischer, C. E. A. Kirschhock and J. A. Martens, *Nanoscale*, Vol. 6 (2014), P. 2056-2060.
- [15] Y. Zhang, J. B. Zhou, X. Chen, Q. Q. Feng, W. Q. Cai, MOF-derived C-doped ZnO composites for enhanced photocatalytic performance under visible light, *J. Alloys. Compd*. Vol. 18 (2018), P. 34086-34092.
- [16] X. B. Yang, L. Q. Qiu, X. T. Luo, ZIF-8 derived Ag-doped ZnO photocatalyst with enhanced photocatalytic activity, *RSC Adv*, Vol. 8 (2018), P. 4890-4894.
- [17] T. J. Whang, M. T. Hsieh, H. H. Chen, Visible-light photocatalytic degradation of methylene blue with laser-induced Ag/ZnO nanoparticles, *Appl. Surf. Sci.*, Vol. 258 (2012), P. 2796-2801.
- [18] C. C. Wang, J. R. Li, X. L. Lv, Photocatalytic Organic Pollutants Degradation in Metal-organic Frameworks. *Energy Environ Sci*, Vol. 7 (2014), P. 2831-2867.

- [19] C. C. Wang, X. D. Du, J. Li J, Photocatalytic Cr(VI) Reduction in Metal-organic Frameworks: A Mini-review. *Applied Catalysis B: Environmental*, Vol. 193 (2016), P. 198-216.